

Size, shape and secondary structure of calponin^{*}

Edward A. Czuryło¹✉, Wolfgang Eimer², Natalia Kulikova¹ and Thomas Hellweg³

¹Nencki Institute of Experimental Biology, Department of Muscle Biochemistry, Warszawa, Poland; ²Universität Bielefeld, Fakultät für Chemie, Physikalische Chemie 1, Bielefeld, F.R.G.; ³TU Chemnitz, Institut für Physik, Materialforschung und Flüssigkeiten, Chemnitz, F.R.G.

Received: 06 June, 2000; accepted: 29 August, 2000

Key words: calponin, circular dichroism, dynamic light scattering, secondary structure estimation, secondary structure prediction

The overall size and shape of the chicken gizzard calponin (CaP) *h1* molecule was investigated by dynamic light scattering (DLS) measurements. From the DLS experiments, a z-averaged translational diffusion coefficient is derived $(5.75 \pm 0.3) \times 10^{-7} \text{ cm}^2 \text{ s}^{-1}$, which corresponds to a hydrodynamic radius of 3.72 nm for calponin. The frictional ratio (1.8 for the unhydrated molecule and 1.5 for the hydrated one) suggests a pronounced anisotropic structure for the molecule. An ellipsoidal model in length 19.4 nm and with a diameter of 2.6 nm used for hydrodynamic calculations was found to reproduce the DLS experimental data. The evaluation of the secondary structure of CaP *h1* from the CD spectra by two independent methods has revealed that it contains, on average, 23% helix, 19% β -strand, 18% β -turns and loops, and 40% of remainder structures. These values are in good agreement with those predicted from the amino-acid sequence. Predictions used for CaP *h1* were applied to other isoforms of known sequences and revealed that all calponins share a common secondary structure. Moreover, the predicted structure of the calponin CH domain is identical to that found by X-ray studies of the spectrin, fimbrin and utrophin CH domains.

Calponin is a thin filament protein present in contractile and cytoskeletal domains as well as in the membrane skeleton of smooth muscle (Mabuchi *et al.*, 1996; North *et al.*, 1994; Small & Gimona, 1998) and nonmuscle

cells expressing smooth muscle protein markers (Lazard *et al.*, 1993; Takeuchi *et al.*, 1991). It was originally found by Takahashi and co-workers (Takahashi *et al.*, 1986; 1988) in chicken gizzard muscle as a troponin-T-like

^{*}Supported by grant from the State Committee for Scientific Research to the Nencki Institute.

✉Corresponding author: Department of Muscle Biochemistry, Nencki Institute of Experimental Biology, L. Pasteura 3, 02-093 Warszawa, Poland; phone: (48 22) 659 8571; fax: (48 22) 822 5342; e-mail: eczurylo@nencki.gov.pl

Abbreviations: CaP *h1*, chicken gizzard calponin *h1* isoform; CH domain, calponin homology domain; CD, circular dichroism; DLS, dynamic light scattering; PHD, the computer algorithm profile network prediction Heidelberg.

protein which binds F-actin, tropomyosin and calmodulin. Later on, it was established that calponin binds myosin (Szymanski & Goyal, 1999; Szymanski & Tao, 1993; 1997) and does not bind to caldesmon – another smooth muscle thin filament constituent (Czuryło *et al.*, 1997b).

The function of calponin is not clear yet. Its ability to inhibit the actin-activated ATPase activity of myosin (Abe *et al.*, 1990; Makuch *et al.*, 1991; Marston, 1991; Winder & Walsh, 1990a) and the movement of actin filaments over immobilized myosin in motility assays (Haerberle, 1994; Kołakowski *et al.*, 1995; Shirinsky *et al.*, 1992) implies that it plays a role in the regulation of smooth muscle contraction (for reviews, see Chalovich & Pfitzer, 1997; Czuryło, 2000; Dąbrowska, 1994; el-Mezgueldi, 1996; Gimona & Small, 1996; Horowitz *et al.*, 1996; Small & Gimona, 1998; Winder *et al.*, 1998). On the other hand, the capability of calponin to interact with the intermediate filament protein, desmin (Wang & Gusev, 1996), tubulin (Fujii & Koizumi, 1999) and to crosslink the actin filaments (Kołakowski *et al.*, 1995; Lu *et al.*, 1995) may suggest its function in cytoskeletal organization. The newest results also add weight to the concept that one of the functions of calponin may be the stabilization of the actin cytoskeleton (Leinweber *et al.*, 1999a). The most intriguing possibility, namely that calponin might have a signaling function, is based on the presence in the calponin structure of the so-called CH domain homologous to those found in signaling proteins (Castresana & Saraste, 1995; Stradal *et al.*, 1998). This idea was confirmed by the observation that the redistribution of calponin coincides with that of protein kinase C (PKC) and mitogen-activated protein kinase (MAPK) (Menice *et al.*, 1997) and that the CH domain of calponin is the region that interacts with extracellular regulated kinase (ERK) (Leinweber *et al.*, 1999b). All the results described above, together with the earlier finding (Nigam *et al.*, 1998) that the absence of *h1*

and *h2* calponins in smooth muscle does not cause any significant loss of contractile activity, suggest that the role of calponin in smooth muscle cells deserves further investigation.

Molecular cloning and sequencing data indicate that there are three calponin isoforms: basic CaP *h1* (pI 8–10), neutral CaP *h2* (pI 7–8) and acidic CaP *ha* (pI 5–6) (Applegate *et al.*, 1994; Strasser *et al.*, 1993; Takahashi & Nadal-Ginard, 1991). Moreover, calponin *h1*, the major species found in adult vertebrate smooth muscle may exist in two isoforms, CaP *h1 α* (formerly called calponin α , molecular mass 32.3 kDa, 292 amino-acid residues) and CaP *h1 β* (formerly called calponin β , molecular mass 28.1 kDa, 252 amino-acid residues) as the result of alternative splicing (Miano *et al.*, 1997; Takahashi & Nadal-Ginard, 1991). The acidic calponin (molecular mass 36.4 kDa, with a C-terminal supplement of about 37 amino acids enriched in acidic residues) was isolated from the vascular smooth muscle rat aorta and non-muscle tissue of adult rat (Applegate *et al.*, 1994; Trabelsi-Terzidis *et al.*, 1995).

Physicochemical studies and electron microscopy of calponin have revealed that its rod-shaped, flexible molecule is approximately 16–22 nm long and has a diameter of about 2.6 nm (Stafford *et al.*, 1995). These authors noted also that there was no distinct difference between naturally occurring calponin *h1* and its *h1 α* isoform expressed in bacteria. Little is known about the calponin secondary structure. The helix content estimated so far from the CD spectra varies from 13% (Stafford *et al.*, 1995) to 41% (Wills *et al.*, 1993) while the value predicted from the sequence analysis is 13% (Takahashi & Nadal-Ginard, 1991). The distribution of the predicted secondary structure elements depends on the procedure applied by the authors and on the calponin source used (Strasser *et al.*, 1993; Takahashi & Nadal-Ginard, 1991).

The aim of this work was to evaluate the complete secondary structure of calponin from CD spectra and primary structure of the

protein, and to calculate its overall size and shape from the dynamic light scattering data. To achieve this, we have applied the methods of Provencher & Glöckner (1981) modified by Venyaminov *et al.* (1993), Hennessey & Johnson (1981), the ALB algorithm (Ptitsyn & Finkelstein, 1983) and the PHD method (Rost & Sander, 1994; Rost *et al.*, 1994) in the secondary structure studies, and the method of Garcia de la Torre & Bloomfield (1981) in the hydrodynamic studies.

MATERIALS AND METHODS

Preparation of calponin. Chicken gizzard calponin was prepared by the original procedure of Takahashi *et al.* (1986) and by the method of Vancompernelle *et al.* (1990) In both cases, the final step of purification consisted of ion-exchange chromatography on an SP-Sephadex column (2.5 cm × 30 cm) which was eluted with a linear (50–300 mM) NaCl gradient either in the presence or absence of 6 M urea. The purified protein was dialysed against 20 mM imidazole buffer, pH 7.0, containing 1 mM EGTA, 1 mM β -mercaptoethanol, 0.02 mM NaN_3 , and a gradually decreasing NaCl concentration (400–100 mM), and then against 50 mM sodium phosphate buffer. The concentration of calponin was determined using the extinction coefficient $E_{275\text{nm}}^{1\%} = 11.3$ (Winder & Walsh, 1990a) and molecular mass 32.3 kDa (Takahashi & Nadal-Ginard, 1991).

CD spectroscopy. The circular dichroism (CD) spectra of calponin *h1* in 50 mM sodium phosphate buffer, pH 7.0, were recorded on an AVIV Model 62DS spectrometer (operated with AVIV 60DS V3.3r software) in the 1 mm-path-length right-angular cell in the far-UV region (180–250 nm) and the 5 mm-path-length right-angular cell in the near-UV region (240–310 nm) over a protein concentration range of 2–9 μM . Before CD measurements, the protein solution was clarified by ultracentrifugation (100 000 × *g*, 45 min). Recording

of each spectrum, including the baseline, was repeated twice. The CD spectra were calculated by averaging the values obtained at different concentrations of five independent batches of calponin prepared by different procedures (see above).

The CD data are presented as molar ellipticity per mean residue mass (Czuryło *et al.*, 1993). Since the difference in mean residue mass of the two calponin isoforms did not exceed 0.8%, the expected spectrum changes had to be much lower than the experimental error. Measurements of CD spectra were carried out at a spectral slit-width of 1.5 nm and time constant set up at 3.0 s. The temperature was either maintained at 20.0 or $80.0 \pm 0.1^\circ\text{C}$, or changed continuously using the manufacturers built-in electronic system. Calibration of the spectrometer wavelength with benzene vapor at 266.71 nm and of the intensity scale with *d*(+)-10-camphorsulfonic acid and epianthrosterone at 290 nm were routinely performed according to the procedures outlined by the manufacturers manual.

Evaluation of the secondary structure from CD spectra. The secondary structure of calponin *h1* was calculated by the extended (Venyaminov *et al.*, 1993) method of Provencher & Glöckner (1981) based on the linear combination of the CD spectra of 16 reference native proteins, 3 denatured proteins and 1 oligopeptide of known structure. It included the constraints $\sum f_i = 1$ and $1 \geq f_i \geq 0$, where f_i denotes the fraction of the *i*-th conformation, i.e.: helix, β -strand, β -turns and remainder structure. Additional evaluation of the secondary structure of calponin was carried out using the orthogonal basic CD spectra method of Hennessey & Johnson (1981) which does not include the constraint $\sum f_i = 1$.

Prediction of secondary structure. The algorithm ALB (Ptitsyn & Finkelstein, 1983) was used for the prediction of secondary structure of all calponin isoforms from their amino-acid sequences. This non-statistical method uses short- and middle-range interactions to predict the secondary structure and

the long-range interactions (in the simplest version of the “floating logs” model) to predict the interactions between the secondary structure elements in question with the hypothetical ones in the tertiary structure. In addition, this algorithm offers the possibility to include the participation of the “real” charge of the macromolecule chain by taking into account the pH, ionic strength and temperature of the environment.

Independently, the publicly available PHD method was used to predict the secondary structure of calponin. This method, which is based on the three-level system of neural networks, was extended by information derived from multiple sequence alignments. This improvement provides higher accuracy of the secondary structure prediction up to 75–88% for a particular structural class of proteins (Rost & Sander, 1994; Rost *et al.*, 1994).

Dynamic light scattering. The intensity I of the light scattered from a dilute macromolecular solution is a fluctuating quantity due to the Brownian motion of the scattering particles. These fluctuations were analyzed in terms of the normalized auto-correlation function $g_1(\tau)$ of the scattered electrical field \mathbf{E}_s , which contains information about the structure and dynamics of the scattering molecules (Berne & Pecora, 1976). Experimentally, the intensity correlation function $g_2(\tau)$ was determined and related to $g_1(\tau)$ by the Siegert relation (Berne & Pecora, 1976):

$$g_2(\tau) = 1 + C |g_1(\tau)|^2 \quad (1)$$

where C is a coherence factor depending on the experimental conditions. For an ideal solution of mono-disperse particles the function $g_1(\tau)$ is represented by a single exponential:

$$g_1(\tau) = \exp(-\Gamma\tau) \quad (2)$$

The relaxation rate Γ is connected to the translational diffusion coefficient D_{exptl} :

$$\Gamma = D_{\text{exptl}} q^2 \quad (3)$$

where q is the scattering vector, $q = ((4\pi n_0)/\lambda)\sin(\Theta/2)$. The scattering vector q depends on the wavelength λ of the incident light and the scattering angle Θ . For polydisperse samples the function $g_1(\tau)$ is given by a weighted sum of exponentials:

$$g_1(\tau) = \int_0^{\infty} G(\Gamma) \exp(-\Gamma\tau) d\Gamma \quad (4)$$

The function $g_1(\tau)$ was analyzed by the method of cumulants (Koppel, 1972) or by the inverse Laplace transformation. These methods provide the mean relaxation rate, $\bar{\Gamma}$, of the distribution function $G(\Gamma)$. For the second analysis procedure mentioned above, the FORTRAN program CONTIN is available (Provencher, 1982a; 1982b). It is sometimes difficult to avoid the presence of spurious amounts of dust particles or high molecular mass impurities that give small contributions to the long time tail of the experimental correlation functions. With CONTIN, it is possible to discriminate these artifacts from the relevant relaxation mode contributing to $g_1(\tau)$.

With the use of eqn. 3, the average apparent translational diffusion coefficient D_{exptl} can be calculated, from the mean relaxation rate, $\bar{\Gamma}$. The measured D_{exptl} depends on the concentration $[C]$ of the scattering particles, and the self-diffusion coefficient D is obtained by extrapolation to zero concentration. This interrelation is usually written as

$$D_{\text{exptl}} = D (1 + k_D [C]) \quad (5)$$

where the diffusional virial coefficient k_D includes the thermodynamic and frictional effects on D (Czuryło *et al.*, 1997a). If the interaction between the particles is negligible, k_D becomes zero and D_{exptl} is equal to D .

Knowing the value of D , the hydrodynamic radius of the scattering particles, R_S , was calculated by the Stokes-Einstein equation

$$D = (kT) / (6\pi\eta R_S) \quad (6)$$

If D has been determined for a protein, it is possible not only to calculate the size of the protein (through the hydrodynamic radius calculated using the Stokes-Einstein equation), but also to compute the frictional ratio f/f_{theo} (with the translational friction coefficients defined by the Stokes equation $f = 6\pi\eta R_S$).

From the frictional ratio, information about the structural anisotropy of the diffusing molecule can be obtained. The ratio of the calculated theoretical hydrodynamic radius $(R_S)_{\text{theo}}$ and the radius R_S obtained from the experiment by using the Stokes-Einstein equation is equal to the ratio of the translational friction coefficients f/f_{theo} :

$$f/f_{\text{theo}} = R_S / (R_S)_{\text{theo}} \quad (7)$$

If the structure of the protein is, in fact, spherical, this ratio equals one. Higher values indicate an anisotropic structure. To obtain this ratio, one must calculate the theoretical hydrodynamic radius $(R_S)_{\text{theo}}$ for the protein under investigation.

Typically, proteins have a mean specific volume of $\nu = 0.73 \text{ cm}^3/\text{g}$ (Eimer *et al.*, 1993). If the molecular mass M is known, a theoretical hydrodynamic radius $(R_S)_{\text{theo}}$ can be estimated using

$$(R_S)_{\text{theo}} = \{(3M\nu) / (4\pi N_A)\}^{1/3} \quad (8)$$

Here, N_A is the Avogadro constant.

Equation 8 is based on the assumption that the investigated molecule is spherical. The diameter of a water molecule is approximately 0.3 nm. By adding this value to the calculated theoretical hydrodynamic radius of the protein, $(R_S)_{\text{theo}}$, hydration is taken into account (Patkowski *et al.*, 1990a; 1990b).

Sample preparation for the DLS measurements. To obtain samples usable for light scattering experiments, calponin was dialyzed against a 20 mM imidazole buffer, pH 7.0, containing 100 mM NaCl, 1 mM EGTA, 1 mM dithiothreitol, and 0.1 mM NaN_3 . The dialysate was refreshed every 2 h over a period of 10–14 h. Afterwards, each solution was clarified by centrifugation for 2 h at $140\,000 \times g$. The concentration of calponin was determined by UV absorption as described above. The protein solutions have been filtered into dust-free sample cells through filters with a pore size of 0.1 μm (Anotop, Whatman). Thereafter, the samples were centrifuged at 10°C for 0.5 h at approximately $1\,000 \times g$. This is necessary to remove larger dust particles and air bubbles. The DLS measurements were carried out at $(10 \pm 0.1)^\circ\text{C}$. The other experimental details and the DLS setup can be found elsewhere (Czuryło *et al.*, 1997a; Patkowski *et al.*, 1990b).

RESULTS AND DISCUSSION

Dynamic light scattering

Two samples of calponin *h1* prepared by each of the two different methods as described in Materials and Methods, were measured at different scattering angles and protein concentrations. The obtained values for the apparent translational diffusion coefficients (Γ/q^2) at different angles were plotted vs the second power of scattering vector (q^2) (Fig. 1). As expected (see eqn. 3), there was no observable angular dependence. This means that only the center of mass diffusion of calponin is monitored and no internal movements contribute to the observed dynamics. The plotted data are mean values over three measurements at each angle. The correlation functions have been analyzed using the CONTIN algorithm (Provencher, 1982a).

The translational diffusion coefficients at $T = 293.15 \text{ K}$ for different calponin concentra-

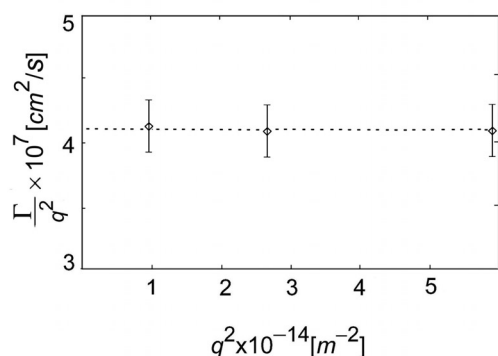


Figure 1. The apparent translational diffusion coefficient (Γ/q^2) of chicken gizzard calponin as a function of the square of the scattering vector (q^2).

The data show a behavior typical for a poorly diffusional relaxation process. The error bars represent an estimated error of 5%.

tions are plotted in Fig. 2. The values in this figure represent an average over three measurements for each protein batch. The values are also an average obtained from measurements for two batches prepared twice by the two methods each. Within experimental accuracy, no significant dependence of the diffusion coefficients on the concentration can be observed (the given error bars correspond to a confidence interval of 95%); therefore we used the mean value calculated from the results for the five different concentrations to proceed in

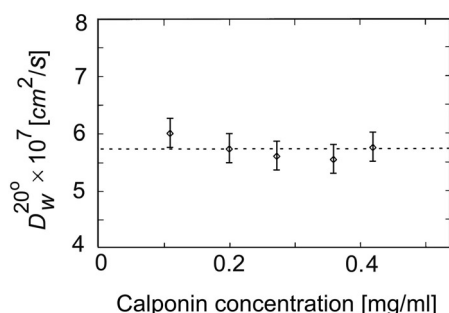


Figure 2. Concentration dependence of the standardized translational diffusion coefficient of calponin hI.

In the used imidazole buffer (see Materials and Methods) no significant concentration dependence is observed. The error bars represent estimated errors of 5%.

our analysis. An interpolation of the data to zero concentration according to eqn. 5 would lead to a slightly higher diffusion coefficient but, within the experimental accuracy, the two results can not be distinguished. Unfortunately, it was difficult to perform the experiments at lower protein concentration because of the low scattering intensity. Using eqn. 6 and the data obtained from the measurements, we have calculated a hydrodynamic radius (R_S) of 3.72 nm for the calponin molecule. Assuming a molecular mass of 32.3 kDa, we calculated a frictional ratio (f/f_0) equal to 1.8 (or 1.55 including a single hydration shell 0.3 nm thick).

So far, there is not much knowledge about the shape of calponin in solution. Stafford and co-workers presented some results obtained by sedimentation studies (Stafford *et al.*, 1995). They calculated a value of 1.33 for the frictional ratio and predicted a prolate ellipsoidal structure for the protein. Our experimental value for the translational diffusion coefficient leads to a somewhat higher value for the frictional ratio. Our values also are in accordance with the structure of a prolate ellipsoid but the molecule seems to be even more anisotropic than calculated by Stafford and co-workers and closer to that observed by electron microscopy (Stafford *et al.*, 1995). From the latter experiments arose a description of the molecule as a prolate ellipsoid of revolutions 16.2 nm long and with a diameter of 2.6 nm. On electron micrographs of calponin, elongated rods with average length of 22 ± 3 nm as well as bent and folded rods were also seen (Stafford *et al.*, 1995) which would rather correspond to the higher frictional ratio calculated by us.

To further clarify the structure of CaP we have performed hydrodynamic model calculations using simple bead models (Garcia de la Torre & Bloomfield, 1981). In Fig. 3, two of these models are shown schematically. The model presented in Fig. 3A corresponds to the structure derived from the sedimentation experiments (Stafford *et al.*, 1995). The ellipsoid

is approximated by 9 beads of different radii. The representation is rather rough and the model has a larger surface accessible to the solvent as compared to the real ellipsoid. This approximation drives the calculated diffusion coefficient towards lower values. The calculations of the translational diffusion coefficient

idealized geometrical objects, which allowed us to perform the best approximation of the observed physical values.

All our results derived from the DLS experiments and those reported by other authors who used various methods are summarized in Table 1.

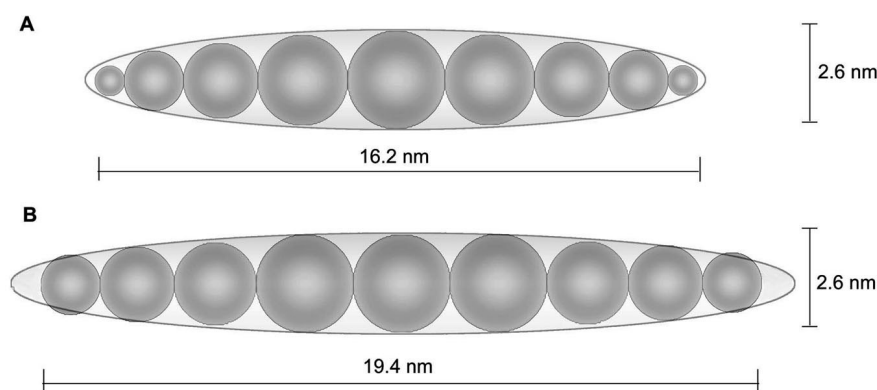


Figure 3. Two models of the calponin molecule approximated by 9 beads.

The radii of the beads from the center to the end are as follows: (A) 1.3, 1.2, 1.0, 0.8 and 0.4 nm and (B) 1.3, 1.3, 1.1, 1.0 and 0.8 nm, respectively.

based on Rotne-Prager tensor (Rotne & Prager, 1969) lead to a value of $7.25 \times 10^{-7} \text{ cm}^2/\text{s}$. This value is significantly larger than the value we have experimentally obtained. Based on the electron micrographs we have constructed another model, presented in Fig. 3B, assuming that the thickness of the molecule is the same and the length is increased to 19.4 nm. For this model we calculated a value of $5.9 \times 10^{-7} \text{ cm}^2/\text{s}$ for the translational diffusion coefficient. Within the experimental error, the calculated translational diffusion coefficient for model B is in good agreement with the results obtained from the DLS experiments (Table 1).

To lower the accessible surface we constructed a third model (not shown), which was built up of overlapping beads with the same axial lengths as in the previous model. The calculated translational diffusion coefficient in this case was $6.1 \times 10^{-7} \text{ cm}^2/\text{s}$. The results obtained from the model calculation indicate that the shape of CaP *h1* molecule in solution is slightly more anisotropic than seen in sedimentation experiments. To avoid a misunderstanding, it should be clarified that both hydrodynamic models shown in Fig. 3 should be treated not as models of a real protein but as

CD spectroscopy. The CD spectra of calponin *h1* recorded at 20°C and 80°C are shown in Fig. 4A. The spectrum recorded at 20°C reveals a double minimum ($[\Theta]_{221} = -7600$ and $[\Theta]_{205} = -12000 \text{ deg} \times \text{cm}^2 \times \text{dmol}^{-1}$) and a maximum ($[\Theta]_{187} = 11000 \text{ deg} \times \text{cm}^2 \times \text{dmol}^{-1}$). The spectrum of calponin measured at 80°C has the same positions of minima, although their negative values are significantly decreased, at ($[\Theta]_{221} = -2600$, and $[\Theta]_{205} = -5100 \text{ deg} \times \text{cm}^2 \times \text{dmol}^{-1}$), thus heating did not cause complete unfolding of calponin.

The mean residue ellipticity at 222 nm as a function of temperature is illustrated in Fig. 4B. The sharp increase in the melting curve in the range of temperatures 40–65°C points to structural transitions occurring in this region. The mid point of these transitions is at 55°C. Above 65°C, the mean residue ellipticity at 222 nm increases linearly up to 80°C. This means that, in this temperature interval, some structural transitions still take place. The first part of the melting curve with a mid point of 57°C was observed earlier by Stafford *et al.* (1995).

Secondary structure estimation and prediction. The results of the estimation of the

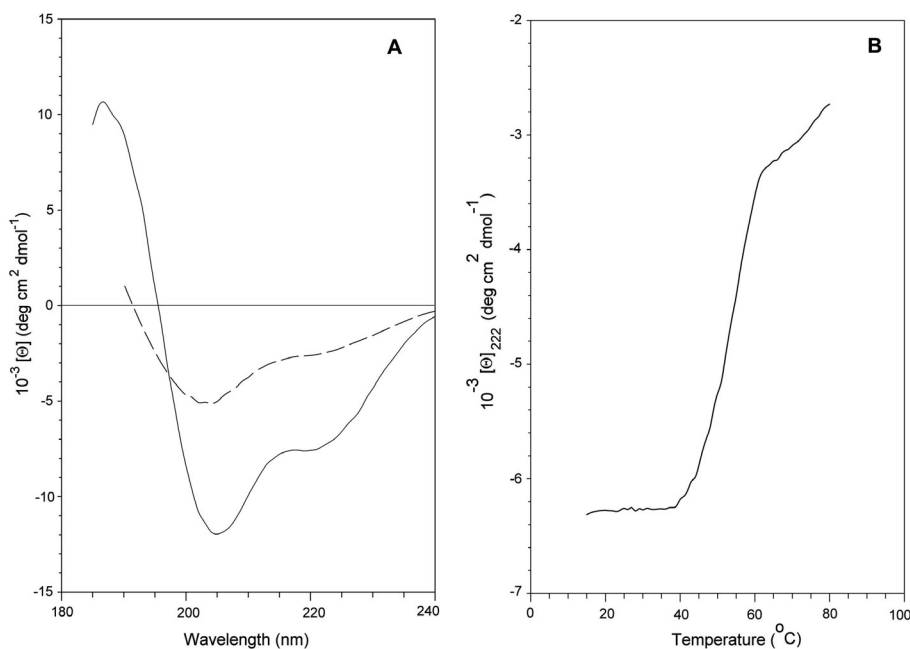
Table 1. The comparison of size and shape parameters of chicken gizzard calponin *h1* isoform determined from dynamic light scattering (DLS) with those taken from the literature

Parameter	DLS	Data from literature
Translational diffusion coefficient	$(5.75 \pm 0.3) \times 10^{-7} \text{ cm}^2 \text{ s}^{-1}$	ND
Sedimentation coefficient	ND	2.34 S (Stafford <i>et al.</i> , 1995) 3.16 S (Takahashi <i>et al.</i> , 1988)
Molecular mass	ND	31400 Da (Stafford <i>et al.</i> , 1995) 32300 Da (Takahashi & Nadal-Ginard, 1991)*
Partial specific volume	ND	0.732 (cm^3/g) (Stafford <i>et al.</i> , 1995) 0.730 (cm^3/g) (Eimer <i>et al.</i> , 1993)*
Hydrodynamic radius	3.72 nm	2.75 nm (Takahashi <i>et al.</i> , 1988)
Frictional ratio for unhydrated molecule	1.8	1.51 (Stafford <i>et al.</i> , 1995)
Frictional ratio for hydrated molecule	1.55	1.32 (Stafford <i>et al.</i> , 1995)
Ellipsoid length	19.4 nm	16.2 nm (Stafford <i>et al.</i> , 1995)
Ellipsoid diameter	2.6 nm	2.6 nm (Stafford <i>et al.</i> , 1995)
Axial ratio	7.46	6.16 (Stafford <i>et al.</i> , 1995)

*Values used in our calculations

secondary structure elements of calponin *h1* from the experimental data shown in Fig. 4A are presented in Table 2 together with the values predicted from the amino-acid sequence.

show that 23% of amino-acid residues of calponin are involved in helical structure, 17% in β -strand, 11% in β -turns, while the rest of the protein (49%) are the remainder struc-

**Figure 4. CD spectroscopy of calponin.**

(A) CD spectra of calponin recorded at 20°C (solid line) and 80°C (dashed line). (B) Thermal transition of calponin. All measurements were performed as described in Materials and Methods.

The estimations according to the modified method of Provencher & Glöckner (1981)

tures. The estimation by the method of Hennessey & Johnson (1981) reveals 23% he-

lix, 22% β -strand, 25% β -turns and 31% remainder structure (Table 2). Thus, except β -turns, the other elements of the secondary structure estimated by these two methods are convergent. Our estimation of the helical structure is almost twice as large as the value (13%) reported by Stafford *et al.* (1995), and

20% of remainder structures (Table 2). It is clear that the ALB algorithm provides a better agreement with the values estimated on the basis of CD spectra, probably because in the structural class of calponin there are no proteins with known structure, which could serve as starting point for the PHD method.

Table 2. Secondary structure of calponin isoforms estimated from CD spectra and predicted from the amino-acid sequence.

Estimations of the secondary structure elements of calponin from CD spectra recorded at different temperatures were performed by the modified method (Venyaninov *et al.*, 1993) of Provencher & Glöckner (P-G) (1981) and by the method of Hennessey & Johnson (H-J) (1981). Predictions were based on the ALB algorithm of Ptitsyn & Finkelstein (P-F) (1983) assuming the existence of interactions between the formed structured segments, and a sequence profile input to neural networks (PHD) (Rost *et al.*, 1994).

Conditions	Secondary structure (%)				Method of estimation or prediction
	Helix	β -Strand	β -Turn and loop	Remainder	
Calponin <i>h1α</i> at 20°C	23	17	11	49	Experimental (P-G)
	23	22	25	31	Experimental (H-J)
	26	14	14	46	Predicted (P-F)
	33	7	40	20	Predicted (PHD)
Calponin <i>h1β</i> at 20°C	30	13	15	42	Predicted (P-F)
Calponin <i>h1α</i> at 80°C	11	36	19	34	Experimental (P-G)
	8	27	15	50	Predicted (P-F)

slightly more than half that (41%) reported by Wills *et al.* (1993). However, in the latter cases, the content of the secondary structure elements of calponin was obtained from CD spectra registered in 100 mM NaCl which, due to shielding by Cl^- ions (Yang *et al.*, 1986), were devoid of about 10 nm in the far UV region. Moreover, the CD spectra of calponin presented by both groups (Stafford *et al.*, 1995; Wills *et al.*, 1993) look similar, so, the differences resulted, most probably, from the estimation method used.

According to the secondary structure prediction based on the amino-acid sequence using the ALB algorithm (Ptitsyn & Finkelstein, 1983), calponin *h1 α* , which is the more abundant isoform of this protein, comprises 26% helix, 14% β -strand, 14% β -turns and loops, and 46% of remainder structures (Table 2). At the same time, the PHD method gives 33% helix, 7% β -strand, 40% β -turns and loops and

The results of prediction obtained with the ALB algorithm for the calponin *h1 β* isoform lacking 40 amino-acid residues (Ala²¹⁷-Gln²⁵⁶, according to the numbering of the amino-acid residues in calponin *h1 α* chain), are as follows: 30% helix, 13% β -strand, 15% β -turns and loops, and 42% of remainder structures. This is very close to the values predicted for calponin *h1 α* . It should be clarified that the numbers of residues involved in helical segments in both isoforms are the same and the higher percentage for the CaP *h1 β* isoform comes from the difference in chain length. For the same reason, the content of β -turns and loops is changed, while the decrease in the content of β -strand results from the decrease in the number of the residues involved in this structure, as some β -strand regions were localized in the part of the chain lacking in the calponin *h1 β* isoform.

Naturally occurring calponin is probably a mixture of isoforms *h1 α* and *h1 β* . The latter isoform is commonly recognized as the minor component, if present at all, while extensive studies with the use of monoclonal antibodies (Jin *et al.*, 1996) did not detect any *h1 β* calponin isoform in various smooth muscle tissues including chicken gizzard. This implies that its expression was absent or at a very low level. Taking into account that the presence of every 5% of *h1 β* isomer in the calponin sample would increase the predicted helix content by 0.2%, then, even for a mixture with 30% of *h1 β* isoform, the increase in helix content by 1.2% is all that could be expected. The changes in other types of structural elements will not exceed the above-presented variations. Changes of such magnitude would slightly impair the agreement of the predicted values with the estimated ones but will stay far from these presented previously (Stafford *et al.*, 1995; Wills *et al.*, 1993).

Heating calponin *h1* to 80°C induced significant alterations in its secondary structure: the content of helical structure decreased by half, the amount of β -strands and β -turns increased and, consequently, the content of the remainder structures decreased (Table 2). The predicted values of all secondary structure elements for the heated calponin are somewhat lower than those estimated from CD spectra.

The probable locations of the helical and β -strand regions of calponin *h1* both at room temperature and at 80°C are presented in Fig. 5. The helical part of calponin is located in the N-terminal region encompassing 135 amino-acid residues and involves 76 residues constituting seven helical segments. Only one helical segment is located at the C-terminal extremity of calponin. Six short β -strand segments (each containing 6–7 amino-acid residues) are dispersed in the second half of the calponin molecule between residues 136 and 280. Takahashi & Nadal-Ginard (1991) found three repeating motifs in the primary sequence of calponin *h1 α* (CLR) starting from residues 164, 204 and 243, respectively (cf.

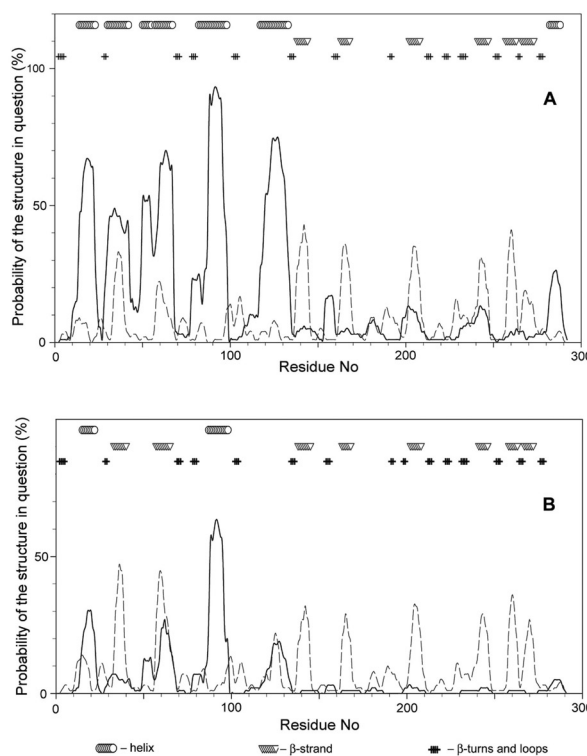


Figure 5. Prediction of the secondary structure elements of calponin *h1* assuming the existence of interactions between the structured segments: (A) at 20°C and (B) at 80°C.

The solid line denotes the probability of helix and the dashed line of β -strand. Amino-acid residues are numbered as described by Takahashi & Nadal-Ginard (1991) and Gong *et al.* (1993).

also Fig. 6). All these units would start with an almost identical β -strand segment if the N-termini of the first and the third motifs were extended by one and of the second by two amino-acid residues. The probability and the location of the helical and β -strand regions in calponin *h1 β* are the same as those for calponin *h1 α* except the fourth β -strand region, which is absent in calponin *h1 β* (not shown).

Each helical segment has a hydrophobic cluster, which suggests its participation in the formation of the hydrophobic core of the protein (Lim, 1978). All β -strand segments have a sequence HxHxHx, where H denotes an amino-acid residue with a large hydrophobic side

chain and x – an amino acid with a polar side chain or glycine. Thus, the β -sheets formed from these segments will have one strongly hydrophobic surface that will interact with, or will be a part of, the hydrophobic core of the calponin *h1* molecule (Lim, 1978). There are many other hydrophobic amino-acid residues in loops. In addition, the number of exposed residues (162) in the calponin molecule is

ing the existence of interactions between the formed structured segments. The results of the prediction of the secondary structure of calponin at high temperature, excluding long-range interactions (the case of the extended state of the polypeptide chain or molten globule state), are close to those at 20°C and far from the experimental ones. Thus, the large amounts of the hydrophobic amino-acid

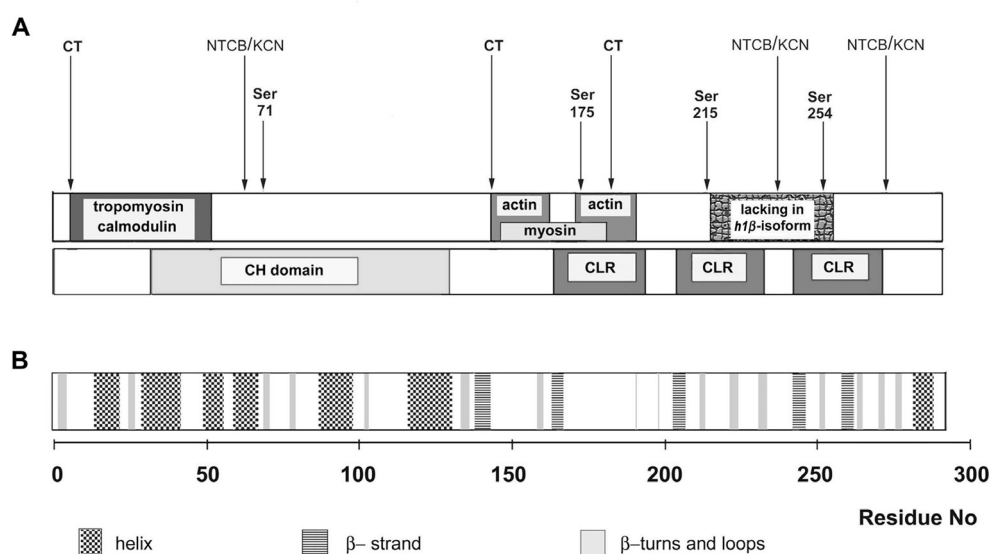


Figure 6. Diagrammatic representation of calponin *h1* molecule.

(A) The binding sites of actin, myosin, tropomyosin, calmodulin, the calponin repeating motifs (CLR) and CH domain are indicated. The sites of chymotryptic (CT) (Mezgueldi *et al.*, 1992) and chemical (NTCB/KCN) (Winder & Walsh, 1990b) cleavages as well as phosphorylatable serines (Winder & Walsh, 1990a) are indicated by arrows. (B) The localization of the secondary structure elements is shown.

much higher than expected (122) for a protein with its molecular mass. All these results taken together seem to indicate that calponin is either an elongated ellipsoid or has a multidomain structure.

The results of the prediction of the probability and location of the secondary structure elements of calponin *h1* at 80°C are shown in Fig. 5B and Table 2. At this temperature, of the segments existing at 20°C, only the first and fifth helical segments and all β -strand segments survived, and three new β -strand segments (two in the N terminus and one in the C terminus of the polypeptide chain) were formed. These results were obtained assum-

residues in calponin (46%), especially of the residues with large hydrophobic side chains (29%), determine the existence of calponin secondary structure at high temperature and its compactness. These results are in good agreement with the observations made in microcalorimetric studies, in which no thermal transition for calponin was observed (D.I. Levitsky, personal communication).

The proposed model of the calponin *h1* secondary structure arrangement (Fig. 6) is consistent with many experimental observations. For example, it explains the different reactivity of the phosphorylation sites; the most reactive Ser¹⁷⁵ (phosphorylated by Ca²⁺/calmo-

dulin-dependent protein kinase II and protein kinase C) (Tang *et al.*, 1996) is located in a relatively long loop between the second and the third β -strand segment, whereas the less reactive serines belong to β -turn (Ser⁷¹) or lie next to a β -turn (Ser²¹⁵ and Ser²⁵⁴). The results of

guanidine hydrochloride and temperature unfolding patterns (see Fig. 5B) are similar).

The procedure used for the prediction of the secondary structure of chicken gizzard CaP *h1* was applied to predict the secondary structure of known isoforms of calponin, the se-

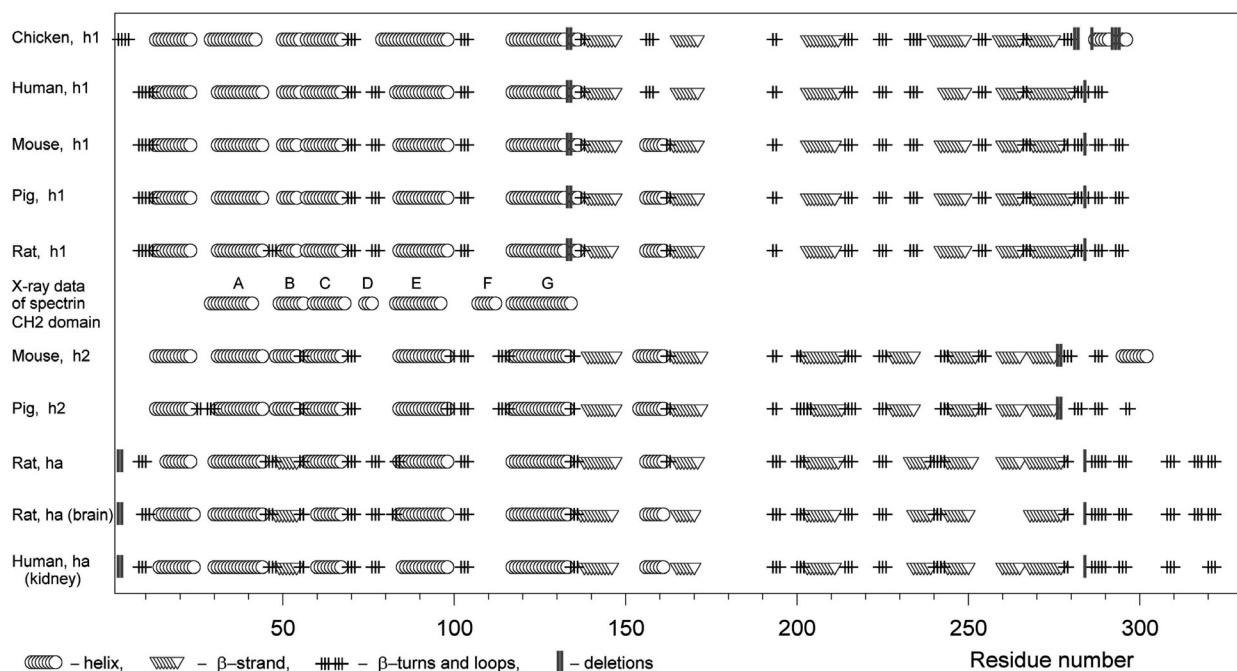


Figure 7. Localization of the secondary structure elements in different calponin isoforms and its comparison with the helical segments (A – G) found in the spectrin CH2 domain and fimbrin or utrophin CH1 and CH2 domains by X-ray crystallography.

proteolytic (Mezgueldi *et al.*, 1992) and chemical (Winder & Walsh, 1990b) cleavages also support the distribution of the secondary structure elements presented in Fig. 6A. The chymotryptic cleavages of calponin take place at amino-acid residues Phe⁶, Tyr¹⁴⁴ and Tyr¹⁸², which are situated in the unstructured regions of the protein. NTCB (2-nitro-5-thiocyanobenzoic acid) attacks primarily the two cysteines (Cys²³⁸ and Cys²⁷³) of calponin located in loops. The extremely low yield of products of cleavage at Cys⁶¹ in the absence and presence of guanidine hydrochloride (Winder & Walsh, 1990b) may be explained by its location in a helical structure or in the β -strand segment surrounded by large and mostly hydrophobic side chains (if the

quences of which are available from data-banks (SWISSPROT and SPTREMBL). All of them have the same pattern of secondary structure (see Fig. 7) regardless of the calponin family, basic (*h1*), neutral (*h2*) or acidic (*ha*), they belong to. Moreover, the parts of the calponin chain representing the CH domain have the same pattern as the CH domains of spectrin, fimbrin and utrophin whose X-ray structures are known (Carugo *et al.*, 1997; Hanein *et al.*, 1998; Keep *et al.*, 1999). The calponin helix corresponding to helix D of the spectrin CH domain is absent because of the deletion in the calponin chain at that position in the sequence alignment. The corresponding helix becomes shorter than four residues and therefore thermodynamically unfavorable.

Thus, structural differences of the CH domain discussed by Keep *et al.* (1999) are undetectable by the CD spectroscopy.

Assuming that the spatial orientation of the calponin helices is close to that observed in the spectrin CH domain, and taking into account the positions of the residues which constitute its hydrophobic core, we could distinguish the residues which form the hydrophobic core of the calponin molecule. These hydrophobic residues are: Leu³⁴, Trp³⁷ and Ile³⁸ (second CaP *h1* helix); Phe⁵⁰, and Leu⁵⁴ (third helix); Ile⁵⁹, Leu⁶⁰ and Leu(Phe)⁶³ (fourth helix) and Val¹²⁰, Leu¹²⁴ and Leu(Val,Ile)¹²⁵ (sixth helix). These residues and their numbering come from the sequence of chicken gizzard calponin but in parentheses are posted the residues met in other calponin isoforms.

The CH domain of calponin has probably been seen on density maps obtained by three dimensional image reconstruction of smooth muscle thin filaments containing calponin (Hodgkinson *et al.*, 1997). The difference density size attributed to calponin is as large as a single actin sub-domain, accounts approximately for one third of the whole calponin mass and equals the mass of its CH domain. Some more difference densities were observed inside the actin area but these parts of difference density may be interpreted either as actin density redistribution after the interaction with calponin or as a contribution of calponin itself. In the latter case, the question arises: is there enough room between the actin monomers to incorporate a part of a calponin molecule? Consequently, is calponin multidomain in solution, or does it change its structure after interaction with actin? It is obvious that the problem of calponin structure needs to be clarified by other methods.

We would like to thank Prof. Renata Dąbrowska for valuable discussion and critical reading of the manuscript.

REFERENCES

- Abe, M., Takahashi, K. & Hiwada, K. (1990) Effect of calponin on actin-activated myosin ATPase activity. *J. Biochem. (Tokyo)* **108**, 835–838.
- Applegate, D., Feng, W., Green, R.S. & Taubman, M.B. (1994) Cloning and expression of a novel acidic calponin isoform from rat aortic vascular smooth muscle. *J. Biol. Chem.* **269**, 10683–10690.
- Berne, B.J. & Pecora, R. (1976) *Dynamic Light Scattering: Applications to Chemistry, Biology, and Physics*; 376 p., John Wiley & Sons, Inc., New York.
- Carugo, K.D., Banuelos, S. & Saraste, M. (1997) Crystal structure of a calponin homology domain. *Nat. Struct. Biol.* **4**, 175–179.
- Castresana, J. & Saraste, M. (1995) Does Vav bind to F-actin through a CH domain? *FEBS Lett.* **374**, 149–151.
- Chalovich, J.M. & Pfitzer, G. (1997) Structure and function of the thin filament proteins of smooth muscle; in *Cellular Aspects of Smooth Muscle Function* (Kao, C.Y. & Carsten, M.E., eds.) pp. 253–287, Cambridge University Press, Cambridge.
- Czuryło, E.A. (2000) Kalponin: biologicheskie, khimicheskie i strukturnie svoistva [Calponin: biological, chemical and structural properties]. *Tsitologiya*. **42**, 7–18 (in Russian).
- Czuryło, E.A., Hellweg, T., Eimer, W. & Dąbrowska, R. (1997a) The size and shape of caldesmon and its fragments in solution studied by dynamic light scattering and hydrodynamic model calculations. *Biophys. J.* **72**, 835–842.
- Czuryło, E.A., Kulikova, N. & Dąbrowska, R. (1997b) Does calponin interact with caldesmon? *J. Biol. Chem.* **272**, 32067–32070.
- Czuryło, E.A., Venyaminov, S.Y. & Dąbrowska, R. (1993) Studies on secondary structure of caldesmon and its C-terminal fragments. *Biochem. J.* **293**, 363–368.
- Dąbrowska, R. (1994) Actin and thin filament-associated proteins in smooth muscle; in *Airways Smooth Muscle: Biochemical Control of*

- Contraction and Relaxation* (Raeburn, D. & Giembycz, M.A., eds.) pp. 31–59, Birkhauser Verlag, Basel.
- Eimer, W., Niermann, M., Eppe, M.A. & Jockusch, B.M. (1993) Molecular shape of vinculin in aqueous solution. *J. Mol. Biol.* **229**, 146–152.
- el-Mezgueldi, M. (1996) Calponin. *Int. J. Biochem. Cell Biol.* **28**, 1185–1189.
- Fujii, T. & Koizumi, Y. (1999) Identification of the binding region of basic calponin on alpha and beta tubulins. *J. Biochem. (Tokyo)* **125**, 869–875.
- Garcia de la Torre, J. & Bloomfield, V.A. (1981) Hydrodynamic properties of complex, rigid biological macromolecules: Theory and application. *Q. Rev. Biophys.* **14**, 81–139.
- Gimona, M. & Small, J. V. (1996) Calponin; in *Biochemistry of Smooth Muscle Contraction* (Barany, M., ed.) pp. 91–103, Academic Press, Inc., San Diego.
- Gong, B.J., Mabuchi, K., Takahashi, K., Nadal-Ginard, B. & Tao, T. (1993) Characterization of wild type and mutant chicken gizzard alpha calponin expressed in *E. coli*. *J. Biochem. (Tokyo)* **114**, 453–456.
- Haeberle, J.R. (1994) Calponin decreases the rate of cross-bridge cycling and increases maximum force production by smooth muscle myosin in an in vitro motility assay. *J. Biol. Chem.* **269**, 12424–12431.
- Hanein, D., Volkmann, N., Goldsmith, S., Michon, A.M., Lehman, W., Craig, R., DeRosier, D., Almo, S. & Matsudaira, P. (1998) An atomic model of fimbrin binding to F-actin and its implications for filament crosslinking and regulation. *Nat. Struct. Biol.* **5**, 787–792.
- Hennessey, J.P., Jr. & Johnson, W.C., Jr. (1981) Information content in the circular dichroism of proteins. *Biochemistry* **20**, 1085–1094.
- Hodgkinson, J.L., el-Mezgueldi, M., Craig, R., Vibert, P., Marston, S.B. & Lehman, W. (1997) 3-D Image reconstruction of reconstituted smooth muscle thin filaments containing calponin: Visualization of interactions between F-actin and calponin. *J. Mol. Biol.* **273**, 150–159.
- Horowitz, A., Menice, C.B., Laporte, R. & Morgan, K.G. (1996) Mechanisms of smooth muscle contraction. *Physiol. Rev.* **76**, 967–1003.
- Jin, J.P., Walsh, M.P., Resek, M.E. & McMartin, G.A. (1996) Expression and epitopic conservation of calponin in different smooth muscles and during development. *Biochem. Cell Biol.* **74**, 187–196.
- Keep, N.H., Norwood, F.L., Moores, C.A., Winder, S.J. & Kendrick-Jones, J. (1999) The 2.0 Å structure of the second calponin homology domain from the actin-binding region of the dystrophin homologue utrophin. *J. Mol. Biol.* **285**, 1257–1264.
- Kołakowski, J., Makuch, R., Stępkowski, D. & Dąbrowska, R. (1995) Interaction of calponin with actin and its functional implications. *Biochem. J.* **306**, 199–204.
- Koppel, D.E. (1972) Analysis of macromolecular polydispersity in intensity correlation spectroscopy: The method of cumulants. *J. Chem. Phys.* **57**, 4814–4820.
- Lazard, D., Sastre, X., Frid, M.G., Glukhova, M.A., Thiery, J.P. & Koteliansky, V.E. (1993) Expression of smooth muscle-specific proteins in myoepithelium and stromal myofibroblasts of normal and malignant human breast tissue. *Proc. Natl. Acad. Sci. U. S. A.* **90**, 999–1003.
- Leinweber, B., Tang, J.X., Stafford, W.F. & Chalovich, J.M. (1999a) Calponin interaction with alpha-actinin-actin: Evidence for a structural role for calponin. *Biophys. J.* **77**, 3208–3217.
- Leinweber, B.D., Leavis, P.C., Grabarek, Z., Wang, C.A. & Morgan, K.G. (1999b) Extracellular regulated kinase (ERK) interaction with actin and the calponin homology (CH) domain of actin-binding proteins. *Biochem. J.* **344**, 117–123.
- Lim, V.I. (1978) Polypeptide chain folding through a highly helical intermediate as a general principle of globular protein structure formation. *FEBS Lett.* **89**, 10–14.
- Lu, F.W., Freedman, M.V. & Chalovich, J.M. (1995) Characterization of calponin binding to actin. *Biochemistry* **34**, 11864–11871.

- Mabuchi, K., Li, Y., Tao, T. & Wang, C.L. (1996) Immunocytochemical localization of caldesmon and calponin in chicken gizzard smooth muscle. *J. Muscle Res. Cell Motil.* **17**, 243–260.
- Makuch, R., Birukov, K., Shirinsky, V. & Dąbrowska, R. (1991) Functional interrelationship between calponin and caldesmon. *Biochem. J.* **280**, 33–38.
- Marston, S.B. (1991) Properties of calponin isolated from sheep aorta thin filaments. *FEBS Lett.* **292**, 179–182.
- Menice, C.B., Hulvershorn, J., Adam, L.P., Wang, C.A. & Morgan, K.G. (1997) Calponin and mitogen-activated protein kinase signaling in differentiated vascular smooth muscle. *J. Biol. Chem.* **272**, 25157–25161.
- Mezgueldi, M., Fattoum, A., Derancourt, J. & Kassab, R. (1992) Mapping of the functional domains in the amino-terminal region of calponin. *J. Biol. Chem.* **267**, 15943–15951.
- Miano, J.M., Krahe, R., Garcia, E., Elliott, J.M. & Olson, E.N. (1997) Expression, genomic structure and high resolution mapping to 19p13.2 of the human smooth muscle cell calponin gene. *Gene* **197**, 215–224.
- Nigam, R., Triggle, C.R. & Jin, J.P. (1998) h1- and h2-calponins are not essential for norepinephrine- or sodium fluoride-induced contraction of rat aortic smooth muscle. *J. Muscle Res. Cell Motil.* **19**, 695–703.
- North, A.J., Gimona, M., Cross, R.A. & Small, J.V. (1994) Calponin is localised in both the contractile apparatus and the cytoskeleton of smooth muscle cells. *J. Cell Sci.* **107**, 437–444.
- Patkowski, A., Eimer, W., Schneider, G., Jokusch, B.M. & Dorfmueller, T. (1990a) The molecular dimensions of G-actin in solution as studied by dynamic light scattering. *Biopolymers* **30**, 1281–1287.
- Patkowski, A., Seils, J., Hinssen, H. & Dorfmueller, T. (1990b) Size, shape parameters, and Ca²⁺-induced conformational change of the gelsolin molecule: A dynamic light scattering study. *Biopolymers* **30**, 427–435.
- Provencher, S.W. (1982a) A constrained regularization method for inverting data represented by linear algebraic or integral equations. *Comput. Phys. Commun.* **27**, 213–217.
- Provencher, S.W. (1982b) Contin: A general purpose constrained regularization program for inverting noisy linear algebraic and integral equations. *Comput. Phys. Commun.* **27**, 229–242.
- Provencher, S.W. & Glöckner, J. (1981) Estimation of globular protein secondary structure from circular dichroism. *Biochemistry* **20**, 33–37.
- Ptitsyn, O.B. & Finkelstein, A.V. (1983) Theory of protein secondary structure and algorithm of its prediction. *Biopolymers* **22**, 15–25.
- Rost, B. & Sander, C. (1994) Combining evolutionary information and neural networks to predict protein secondary structure. *Proteins* **19**, 55–72.
- Rost, B., Sander, C. & Schneider, R. (1994) Redefining the goals of protein secondary structure prediction. *J. Mol. Biol.* **235**, 13–26.
- Rotne, J. & Prager, S. (1969) Vibrational treatment of hydrodynamic interaction in polymer. *J. Chem. Phys.* **50**, 4831–4837.
- Shirinsky, V.P., Biryukov, K.G., Hettasch, J.M. & Sellers, J.R. (1992) Inhibition of the relative movement of actin and myosin by caldesmon and calponin. *J. Biol. Chem.* **267**, 15886–15892.
- Small, J.V. & Gimona, M. (1998) The cytoskeleton of the vertebrate smooth muscle cell. *Acta Physiol. Scand.* **164**, 341–348.
- Stafford, W.F., Mabuchi, K., Takahashi, K. & Tao, T. (1995) Physical characterization of calponin. A circular dichroism, analytical ultracentrifuge, and electron microscopy study. *J. Biol. Chem.* **270**, 10576–10579.
- Stradal, T., Kranewitter, W., Winder, S.J. & Gimona, M. (1998) CH domains revisited. *FEBS Lett.* **431**, 134–137.
- Strasser, P., Gimona, M., Moessler, H., Herzog, M. & Small, J.V. (1993) Mammalian calponin. Identification and expression of genetic variants. *FEBS Lett.* **330**, 13–18.

- Szymanski, P.T. & Goyal, R.K. (1999) Calponin binds to the 20-kilodalton regulatory light chain of myosin. *Biochemistry* **38**, 3778–3784.
- Szymanski, P.T. & Tao, T. (1993) Interaction between calponin and smooth muscle myosin. *FEBS Lett.* **334**, 379–382.
- Szymanski, P.T. & Tao, T. (1997) Localization of protein regions involved in the interaction between calponin and myosin. *J. Biol. Chem.* **272**, 11142–11146.
- Takahashi, K., Hiwada, K. & Kokubu, T. (1986) Isolation and characterization of a 34 000-dalton calmodulin- and F-actin-binding protein from chicken gizzard smooth muscle. *Biochem. Biophys. Res. Commun.* **141**, 20–26.
- Takahashi, K., Hiwada, K. & Kokubu, T. (1988) Vascular smooth muscle calponin. A novel troponin T-like protein. *Hypertension* **11**, 620–626.
- Takahashi, K. & Nadal-Ginard, B. (1991) Molecular cloning and sequence analysis of smooth muscle calponin. *J. Biol. Chem.* **266**, 13284–13288.
- Takeuchi, K., Takahashi, K., Abe, M., Nishida, W., Hiwada, K., Nabeya, T. & Maruyama, K. (1991) Co-localization of immunoreactive forms of calponin with actin cytoskeleton in platelets, fibroblasts, and vascular smooth muscle. *J. Biochem. (Tokyo)* **109**, 311–316.
- Tang, D.C., Kang, H.M., Jin, J.P., Fraser, E.D. & Walsh, M.P. (1996) Structure-function relations of smooth muscle calponin. The critical role of serine 175. *J. Biol. Chem.* **271**, 8605–8611.
- Trabelsi-Terzidis, H., Fattoum, A., Represa, A., Dessi, F., Ben-Ari, Y. & Der Terrossian, E. (1995) Expression of an acidic isoform of calponin in rat brain: Western blots on one- or two-dimensional gels and immunolocalization in cultured cells. *Biochem. J.* **306**, 211–215.
- Vancompernelle, K., Gimona, M., Herzog, M., Van Damme, J., Vandekerckhove, J. & Small, V. (1990) Isolation and sequence of a tropomyosin-binding fragment of turkey gizzard calponin. *FEBS Lett.* **274**, 146–150.
- Venyaminov, S., Baikalov, I.A., Shen, Z.M., Wu, C.S. & Yang, J.T. (1993) Circular dichroic analysis of denatured proteins: Inclusion of denatured proteins in the reference set. *Anal. Biochem.* **214**, 17–24.
- Wang, P. & Gusev, N.B. (1996) Interaction of smooth muscle calponin and desmin. *FEBS Lett.* **392**, 255–258.
- Wills, F.L., McCubbin, W.D. & Kay, C.M. (1993) Characterization of the smooth muscle calponin and calmodulin complex. *Biochemistry* **32**, 2321–2328.
- Winder, S.J., Allen, B.G., Clement-Chomienne, O. & Walsh, M.P. (1998) Regulation of smooth muscle actin-myosin interaction and force by calponin. *Acta Physiol. Scand.* **164**, 415–426.
- Winder, S.J. & Walsh, M.P. (1990a) Smooth muscle calponin. Inhibition of actomyosin MgATPase and regulation by phosphorylation. *J. Biol. Chem.* **265**, 10148–10155.
- Winder, S.J. & Walsh, M.P. (1990b) Structural and functional characterization of calponin fragments. *Biochem. Int.* **22**, 335–341.
- Yang, J.Y., Wu, C.-S.C. & Martinez, H.M. (1986) Calculation of protein conformation from circular dichroism. *Methods Enzymol.* **130**, 208–269.